PHOTOCLINOMETRIC ANALYSIS OF RESURFACED REGIONS ON EUROPA. C. Thomas & L. Wilson. Planetary Science Research Group, Environmental Science Dept., Institute of Environmental and Natural Sciences, Lancaster University, Lancaster LA1 4YQ, England. constantine.thomas@lancaster.ac.uk.

Introduction: The Galileo Solid State Imaging (SSI) camera imaged a region of Europa centred at 5.73°N 326.54°W at a resolution of 25.3 metres per pixel (50.6 metres per line pair) during the E4 flyby through the Jovian system as part of the E4ESDRKMAT02 observation. The imaged area (c0374685452r.img) is located on the subjovian hemisphere in a region previously observed only at very low (< 5 km) resolution by Voyager and at 330 metre resolution in other E4 Galileo images.

The imaged region is characterised by complex sets of criss-crossing fractures, multiple and doublet ridges in various orientations characterised as 'washboard plains' [1]. The surface on which these ridges are located is broken up in many places around this area, and there is evidence for lateral movement of 'rafts' of surface material similar to that interpreted in the Chaos terrains imaged on other orbits [1] elsewhere in the E4ESDRKMAT02 observation.

There are at least three examples in c0374685452r.img of terrain that is locally smoother than its surroundings, and these are interpreted here as the result of resurfacing events that have covered underlying material [1]. These areas are irregular in shape and closely follow ridge boundaries.

One particular area - a roughly elliptical feature referred to henceforth as the 'pond' given its appearance [2] (shown in Figure 1) - is the subject of analysis in this abstract. Since ridges to the north and south of the pond are submerged by it, it is possible to determine the depth of the pond if the height of the submerged ridges is known. To this end, topographic profiles of the area within and around the pond were derived using photoclinometry. The pond morphology (also derived partly from photoclinometry) and the resulting implications for the rheology and nature of the erupted fluid are described.

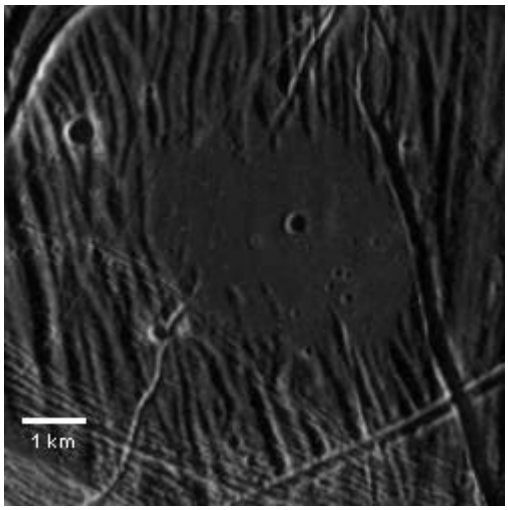

Figure 1: Pond-like feature imaged by Galileo.

Morphology: The smooth pond covers an area of approximately 6.5 x 10^6 m^2; it can be roughly approximated by a 3700 m x 1240 m ellipse. Its albedo is low and similar to that of surrounding terrain which is comprised of dense interleaving N-S trending sinuous ridges and troughs. The relief of these features is low, though some high-standing ridges are present to the south of the pond.

The pond itself appears regionally smooth, though this conclusion is reinforced by the presence of large (8x8) pixel image compression artifacts that serve to average out the DNs in the region. Small impact craters between 50 and 125 m in diameter are present in the pond's southeastern quadrant, and a relatively large circular crater with a diameter of 250 m is located (coincidentally?) near the centre of the pond. The only other structures visible in the pond are what appear to be the tops of broad ridges that enter it from the north and south.

The smooth, flat appearance of the area covered by the pond contrasts with the obvious topographic variation of the ridged terrain surrounding it, indicating that the pond material was rapidly emplaced as a fluid that submerged pre-existing topography to varying degrees. This suggests a high effusion rate from an as-yet unidentified source probably hidden beneath the pond material.

The pond material covers low-lying regions between the ridges impinging on it, mainly on the northern and southern edges where the ridges are perpendicular to the pond margin. Ridges disappear towards the centre of the pond, indicating that it is deepest there. However, since ridge traces are still visible in this central region, the maximum depth of the pond cannot be that much greater than the maximum height of the ridges it covers; these heights are derived in the photoclinometric analysis below so that a minimum volume of the pond can be calculated. The eastern and western margins of the feature are more nearly parallel to (and therefore follow) the ridged surface texture.

The eastern border of the pond is marked by a 200 m wide fracture that braids to the north, the western rim of which has a 'fuzzy' appearance interpreted here as pond overflow into the fracture when the pond material was erupted. A 100 m wide NE-SW fracture traverses (but disappears into) the pond. The pond is stratigraphically the youngest unit in the imaged region since it floods or embays all the fractures and ridges that impinge on it.

There are neither obvious flow fronts within the pond nor any levees along its margins visible at the resolution of the image. This sets the maximum height of any levees that do exist to no greater than a few metres, limiting the maximum yield strength of the pond material (if it was indeed erupted as a non-Newtonian fluid) to << 10 Pa.

Image Preparation: To prepare the image for photoclinometric analysis, it was first calibrated and then reprojected (using the USGS ISIS software package) to a sinusoidal reprojection centred on the central crater in the pond. The image was then output from ISIS as a raw image with the DN range determined by the DSK2DSK program, which determines the full range of DNs contained in the image.

The reprojection process always rotates the raw image so that north is directly 'up' in the reprojected image, so the reprojected image should be further rotated such that the solar illumination is coming directly from the right of the image in order to maximise the accuracy of the profiles. All illumination and orientation information is acquired from the image labels, and it is necessary to assume that it is completely accurate - given the current lack of accurate SPICE pointing data for Europa this may not be the case. Furthermore, it should be noted that rotating the image may introduce resampling errors (attributing slightly different DNs to pixels from those that they possess in the original calibrated image), though the reprojection process itself is likely to introduce errors as it reprojects and rotates the original calibrated image. Furthermore, image compression blocks in the image are (ironically) concentrated in the smooth areas such as the pond and may cause errors since the actual terrain pixels are subsumed into the compression artifact. However, while these errors may affect the outcome of the photoclinometry process it is unlikely that they are very significant and they will certainly not affect the broad shape of the profile.

Photoclinometric analysis: The aim of the photoclinometric analysis of the pond area performed here is to determine the maximum height of the ridges that are submerged by the pond in order to estimate a lower bound for its depth and volume.

As there is no evidence in large-scale mosaics of this area to suggest a regional east-west slope across this locality [1], a regionally flat 'background' surface for the area can be assumed here. Each profile was derived using a range of possible pixel DN values that could potentially correspond to locally flat surfaces in the analysed row

of the image. The topographic slope between adjacent pixels is derived by taking the ratio of the DN of each pixel to a DN value that corresponds to a flat surface appropriate to that terrain type (the latter is known as the Flat Surface DN, or FSDN). By interpreting this ratio in terms of a chosen photoclinometric function using techniques similar to those described in [3], the slope corresponding to the brightness difference can be calculated across a horizontal distance equal to the image resolution (25.3 m/pxl in this case) - the higher the ratio, the steeper the slope.

It is assumed that the pond surface is itself an approximately flat and level plane. Thus profiles that are generated across the pond surface that are not flat and level must not use an appropriate assumed FSDN. If an assumed FSDN across a row is too high, the sun-facing slopes are shallower than expected while those facing away from the sun are steeper, resulting in skewed topography and an artificial sun-facing regional slope across the profile. Since the incident illumination in the image is from the right of the image, this means that the terrain on the left edge of the pond would appear much lower than the terrain on the right edge of the pond - the inverse applies if the chosen FSDN is too low. Those FSDN values that yielded such unreasonable slopes could be and were discarded, leaving a much smaller range of more reasonable FSDN values that could be used in the analysis. The most appropriate FSDN was then picked out from this reduced range using the image as a guide and used to generate the final profile for that row.

This FSDN was then used in a second profile-generating program where the FSDN could be varied across the profile. This could be used to 'fine-tune' the profile in various ways and could also be used to more accurately determine the absolute albedoes of the features in the profile since the FSDN is directly proportional to the albedo. Craters are assumed to have opposite rims at the same height, so if they appeared at different heights in the profile the FSDN across the crater could be tweaked until they were the same - this would then yield an optimum estimate for the FSDN of the crater. Symmetrical-looking ridges on the pond are another feature than can be adjusted in this way - if the ridge FSDN were too high or low it would result in an asymmetrical ridge on the profile and a height difference in the pond on either side of the ridge. The FSDN of the ridge can be adjusted so that the ridge becomes symmetrical in profile and the pond becomes level, and the albedo of the ridge can then be determined.

Several assumptions are made about the topography of features in the pond region - that craters (most of those found in the image appear to be bowl-shaped) have rims that are the same height, that any ridges are symmetrical in profile along their axes relative to the surface that they are on (e.g. a 'double ridge' is assumed to consist of two symmetrical side-by-side ridges with triangular cross-section). While these assumptions may not be strictly realistic they appear to be generally supported by visual interpretation of the image and so serve as a good starting point for this analysis.

Preliminary topographic profiles were derived in this way across the pond and the ridges to its north and south, using visual interpretation as an aid. In addition, albedo effects can significantly alter derived slope values by artificially increasing or decreasing the DN values expected from topography alone - however, these are generally noticeable in the profiles as isolated examples of anomalously steep slopes (such as those found on the bright sun-facing walls of some ridges and troughs).

The shapes of the profiles are determined by the photometric function used. Obviously, this has to match that of the surface if the profiles are to be completely accurate. The most detailed and accurate photometric function is the Hapke function but this is extremely complicated, containing many terms (e.g. pore size between grains of material on the surface) that can only be guessed at, and it is computationally very difficult to incorporate into a profile-generating program such as the one used here. There is one function - the Lommel-Seeliger function - that is essentially a 'distillation' of the Hapke function that does not contain the more complicated terms. The Lommel-Seeliger function relies on the incidence and emergence angles alone, and since it is directly related to the Hapke function it is the one used here. There are other functions - the Lambert (incidence angle dependence only) and the Minnaert, but these functions are not simply related to the Hapke and are therefore less likely to be appropriate. The Lambert and Lommel-Seeliger functions represent end-members on a scale that ranges from an 'icy-type' surface (Lambert) to a 'lunar-type' surface (Lommel-Seeliger). It should be noted that any phase-angle dependence of these functions is not relevant when generating topographic profiles, since the phase angle within a single image is effectively the same anywhere within the image area. Further development of the program used to derive these profiles is anticipated to allow the use of more accurate photometric functions.

Results: Since the pond itself is interpreted as being flat and with no regional slope, the FSDN across that region can be assumed to be the same as the average DN over the entire area covered. At least two such appropriate 'initial FSDNs' were derived; one for pond material (FSDN 35), the other for the ridges to the north and south (FSDN 40). However, it was found to be difficult to constrain the FSDN to a single value along the profiles - in some cases up to ten different values were used along a profile, though within the pond these rarely varied by ± 3 DN at most. For example, the crater at the centre of the pond was found to require a higher FSDN (40) than the surrounding pond material in order to keep the opposite rims at the same height, although this may be more due to the fact that most of the crater diameter is occupied by shadow. As expected, the pond material FSDN value was found to be lower than that of the surrounding ridges.

The observed morphology of the northern and southern pond margins results from low relief ridges gradually sloping downwards towards the centre of the pond; those ridges that are locally taller are more likely to stand out above the pond surface closer to the centre, and small-scale variations in the angle of slope beneath the pond could also result in lower relief ridges protruding from the surface nearer the centre.

The heights of ridges to the north and south of the pond are consistently found using the photoclinometric techniques described here to lie between 10 and 30 metres above the surrounding terrain - all of these are eventually completely submerged within the pond itself. Work in ongoing to verify these results with more profiles across the area.

Since it is possible to see traces of ridges continuing through the pond at least part of the way across the feature, the pond is unlikely to be greater than 50 metres deep at most, and is most likely to be roughly parabolic in cross-section so that the ridge tops can remain close to the surface for their traces to be visible. Using this depth, the maximum volume of material erupted to form the pond is therefore approximately 0.35 km^3.

References: [1] J. W. Head et al. (1998) In LPSC XXIX, Abstract #1412, LPI, Houston. [2] J. W. Head et al. (1998) In LPSC XXIX, Abstract #1491, LPI, Houston. [3] Mouginis-Mark, P.J. & Wilson, L. (1981) MERC: a FORTRAN IV program for the production of topographic data for the planet Mercury. Comp. Geosci. **7**, 35-45.